

## Article

# Planform Dynamics and Cut-Off Processes in the Lower Ucayali River, Peruvian Amazon

Jorge D. Abad <sup>1,\*</sup> , Alejandro Mendoza <sup>2</sup>, Kristin Arceo <sup>3,†</sup>, Zara Torres <sup>4,‡</sup>, Henry Valverde <sup>5</sup>, Gerles Medina <sup>5</sup>, Christian Frias <sup>6</sup> and Moisés Berezowsky <sup>2</sup>

<sup>1</sup> Department of Research, Education and Development, RED YAKU, Lima 15084, Peru

<sup>2</sup> Instituto de Ingeniería, Universidad Nacional Autónoma de México, México 04510, México

<sup>3</sup> Department of Civil and Environmental Engineering, University of Pittsburgh, Pittsburgh, PA 15261, USA

<sup>4</sup> Facultad de Agronomía, Universidad Nacional de la Amazonía Peruana, Iquitos 16002, Peru

<sup>5</sup> Department of Civil Engineering, University of Engineering and Technology, Lima 15063, Peru

<sup>6</sup> Barr Engineering Co., Minneapolis, MN 55435, USA

\* Correspondence: jabad@redyaku.com

† Current address: AECOM, Pittsburgh, PA 15219, USA

‡ Current address: Social Development and Compensation Fund Project—FONCODES, Lima 15046, Peru

**Abstract:** The Ucayali River is one of the most dynamic large rivers in the world, with high rates of channel migration regularly producing cutoffs. In the lower portion of the Ucayali River, before its confluence to the Marañon River where the Amazon River is born, the increase in water and sediment discharge triggers bends with secondary channels (transitional stage from purely meandering to anabranching), which influence the planform migration rates and patterns of the sinuous channels. Based on remote sensing analysis, a comparison of planform dynamics of bends with and without secondary channels is presented. For the case of a bend with secondary channels (Jenaro Herrera, JH), detailed field measurements for bed morphology, hydrodynamics, bed and suspended load are performed for low-, transitional- and high-flow conditions (August, February and May, respectively). Additionally, a two-dimensional depth average hydraulic model is utilized to correlate observed migrating patterns with the hydrodynamics. Results indicate that the secondary channels have disrupted typical planform migration rates of the main meandering channel. However, at high amplitudes, these secondary channels reduce their capacity to capture flow and start a narrowing process, which in turn increases migration rates of the main channels (meandering reactivation process), suggesting that an imminent cutoff along the JH bend is underway by pure lateral migration or by the collapse into the existing paleochannels.

**Keywords:** Ucayali River; neck cutoff; Jenaro Herrera bend



**Citation:** Abad, J.D.; Mendoza, A.; Arceo, K.; Torres, Z.; Valverde, H.; Medina, G.; Frias, C.; Berezowsky, M. Planform Dynamics and Cut-Off Processes in the Lower Ucayali River, Peruvian Amazon. *Water* **2022**, *14*, 3059. <https://doi.org/10.3390/w14193059>

Academic Editors: Edgardo M. Latrubesse, Karla M. Silva de Farias and Maximiliano Bayer

Received: 23 August 2022

Accepted: 20 September 2022

Published: 28 September 2022

**Publisher's Note:** MDPI stays neutral with regard to jurisdictional claims in published maps and institutional affiliations.



**Copyright:** © 2022 by the authors. Licensee MDPI, Basel, Switzerland. This article is an open access article distributed under the terms and conditions of the Creative Commons Attribution (CC BY) license (<https://creativecommons.org/licenses/by/4.0/>).

## 1. Introduction

The Ucayali River is a large meandering river in the Peruvian Amazon Basin that drains an area of 360,000 km<sup>2</sup> [1,2]. It carries one of the highest suspended sediment loads of any of the tributaries to the Amazon River [3–5]. In terms of planform migration, the Ucayali is one of the most active rivers in the Amazon Basin, where oxbow lakes, neck and chute cutoffs are common [2,4,6,7]. Past studies have calculated the migration rates of bends (at the apex) in this river to be on average 60–80 m/year, with maximum migration rates reaching 150 m/year, while migration rates on reaches between the apex and the inflection point of a meander averaged around 25 m/year [2,4,8]. The Ucayali River has been important to the people that have populated its valley for thousands of years, due to the fertile soils along the floodplain, fishing, and the connectivity that it provides to other communities; the river still plays a vital role today for these same reasons, as regional roads are minimal—ninety percent of cargo and passenger traffic in the department containing the lower Ucayali River is on the fluvial network [7,9]. However,

unlike traditional transportation networks, the distance of travel between two points on the Ucayali River changes over time due to migration of the river and the occurrence of cutoff channels. Cutoff processes play an important role in meandering river dynamics by reducing the complexity of a particular reach and also by acting as a noise that changes the dynamics of the river on a whole; thus, it is important to maintain the steady state of a river. Therefore, in the long term, the river maintains a dynamic steady state of geomorphic characteristics [10,11]. There are two types of cutoffs. In neck cutoffs, the sinuosity and tortuosity of the bend become so high that the water crosses the narrow neck, resulting in the two limbs effectively “colliding” [11,12]. In chute cutoffs, which typically occur in wide channels with large curvature, high discharges, high gradients, and poorly cohesive, weakly vegetated banks, a new channel is cut across the neck of a meander bend during floods that reduces sinuosity [11,13–15]; ref. [10] specify that a channel in a chute cutoff is “relatively long”; similarly, ref. [16] only consider cutoffs that occur at a distance greater than one channel-width as a chute cutoff, while [14] consider any process in which a new channel is incised as a chute cutoff. Herein, the definition of chute cutoff provided by [14] is used. Predicting chute cutoffs remains an unresolved problem, but it may be an important process for long-term sediment flux [10,17]. When a neck cutoff occurs, oxbow lakes are formed once the old channel becomes closed by sedimentation [10,18]. While a cutoff may reduce travel time for people using the river waterways, it can also lead to increased flooding risk downstream of the cutoff and the isolation of towns from their source of fishing, sites for planting crops, and the fluvial transportation network [19,20]. Along the Ucayali River, there is evidence of several oxbow lakes that were formed between 3000 to 3540 cal yr BP [21]. Ref. [22] analyzed the Ucayali River from 1985 to 2015 and found around 42 cutoffs (chutes and necks), and [22] analyzed processes with nonlinearities along the Ucayali River. Ref. [23] described the adaptation processes (upstream and downstream migration and channel widening) when meander cutoffs occurred along the Ucayali River. Similar processes for this river were previously discussed by [24].

In the Lower Ucayali River (Figure 1), two recent cutoffs occurred in the past twenty years, named herein as US and DS, and one more bend, Jenaro-Herrera (JH), appears to be under pre-cutoff conditions. From Figure 1, it is observed that the Ucayali River is very active, as the presence of paleochannels, scroll bars, and oxbow lakes along the river valley indicate. Indeed, ref. [25] has shown that the Ucayali River is responsible for the connectivity between river geomorphology and biodiversity in the Ucamara depression. This study aims to understand pre-existing conditions of the JH bend by temporal analysis of Landsat images and a numerical model paired with detailed field measurements. Typically, small towns living near the river relocate as the river migrates; however, the town of Jenaro Herrera, founded in 1954, is located on the apex of the bend and has around 5100 people, a relative large number in the region, and there is infrastructure that is difficult to displace (e.g., a school, an experimental research center, and roads) that might not allow the town to follow the Ucayali River. Rather, authorities might need to plan the logistics to develop projects related to access navigation, sewage system, and other economical activities in advance, foreseeing the future river migration.

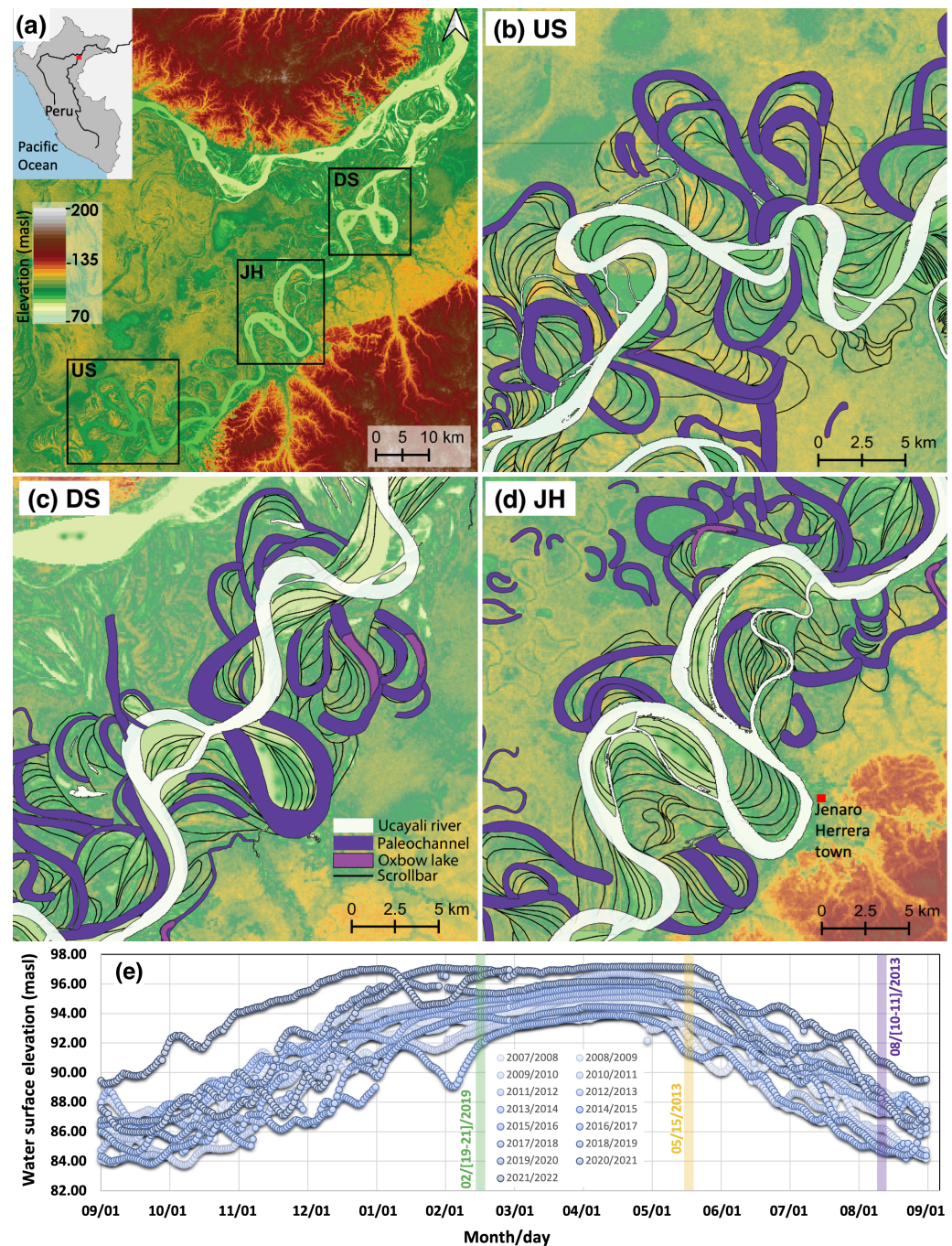


**Figure 1.** (a) The Ucayali depression (see the DEM) where the Ucayali River (meandering) meets the Marañón River (anabranching) to form the Amazon River (anabranching); (b) upstream (US) bend; (c) downstream (DS) bend; (d) the Jenaro Herrera (JH) bend along the Ucayali River. In (b–d) the main channel of the Ucayali River is shown as well as the reconstruction of paleochannels and oxbow lakes, describing the planimetric dynamic of the Ucayali River throughout time. For dynamics on the confluence between the Ucayali and Marañón Rivers, see [26], (e): the water surface elevation (m) at the Jenaro Herrera gauging station from 2007 to 2021. Shaded regions denote the field measurement campaigns in May and August 2013 and February 2019.

## 2. Cutoffs near Jenaro-Herrera Town

In order to gain an understanding of the channel migration and cutoff processes in this reach of the Ucayali River near Jenaro Herrera town, a temporal analysis for recent bend cutoffs on the lower Ucayali has been performed. The temporal analysis was based on Landsat images, which have a resolution of 30 m ([glovis.usgs.gov](http://glovis.usgs.gov), accessed on 30 June

2022). Planform characteristics were calculated with mStaT, [27] for these bends in order to determine if there are any common factors in the cutoff processes. Figures 2–4 show the changes in these bends (US, JH, and DS) from 1987 to 2020.

### 2.1. Upstream (US) Bend

The neck cutoff of the US bend (see Figure 2a) took place between September and December of 1990 (see Figure 2b). The US bend elongated significantly before the neck cutoff occurred, and a secondary channel similar to a chute cutoff was present in the bend. The upstream limb of the bend had a high sinuosity, and proceeded to collide into the downstream limb, which had a low sinuosity reach and was migrating at a lower rate.

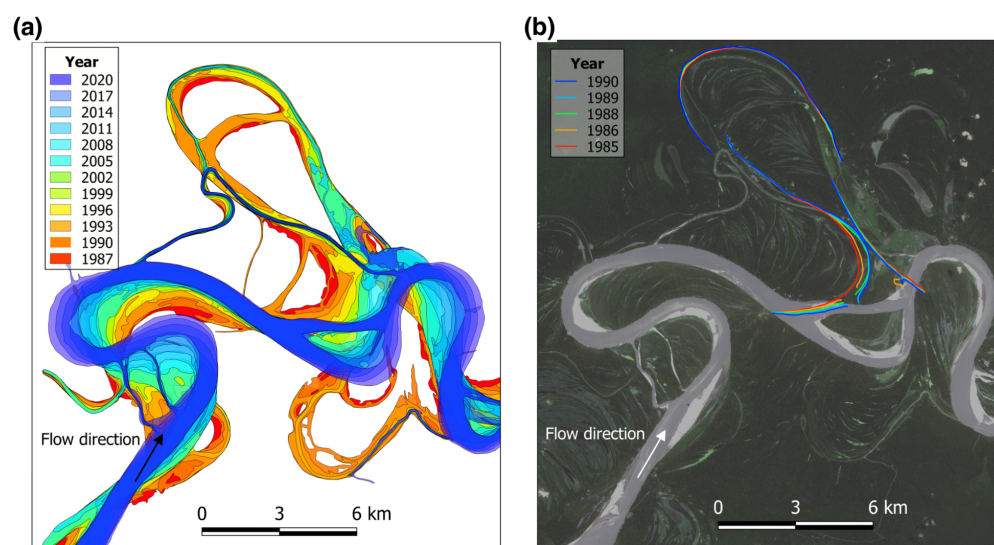


**Figure 2.** (a) Planform migration of the US bend (see Figure 1 for location) from 1987 to 2020. (b) The migration of the outer bank from 1985 to 1990, the interval when the neck cutoff occurred.

This collision created a channel connection with a width approximately equal to the main channel width. By April 1991, the colors of the water in the new and old channels were different, indicating that the sediment concentration was different in these two portions of the channel and the water was flowing through the new channel and had abandoned the old channel, even though they still shared connectivity. By September 1995, the old channel had been completely abandoned on the upstream end, but there was still connectivity from a small channel. After the bend was abandoned, the new bend began a process of downstream translation, as expected in the early stages of a meander bend development [28].

### 2.2. Jenaro Herrera (JH) Bend

The JH bend (see Figure 3a,b), despite its high sinuosity, has not shown as much activity as the US and DS bends. The JH bend appears to cross a fault, and the reach near the apex, which is about 10 km long, borders the Upper Nauta and Ucamara formations instead of just alluvial deposits [29]. The lower Ucayali River is near the Brazilian Craton with an escarpment that borders the downstream portion of the JH bend [29,30]. The JH bend has secondary channels (as observed in Figure 3) that formerly were the main channel (wider channels, especially upstream of Jenaro Herrera town). However, due to a planform reconfiguration, on the one hand, the main channel is becoming more elongated and sinuous, and on the other hand, the secondary channels are undergoing a narrowing process (the trapping efficiency of water and sediments are being reduced). The loop on the upstream reach (Figure 3b) of the JH bend has become more rounded over the past years, with a larger radius of curvature, and has migrated downstream towards the downstream loop. The downstream reach (Figure 3b) has also migrated towards the upstream loop at its apex, but to a smaller degree because of the downstream translation of the entire

bend. It seems that a cutoff might occur with the collision of the upper and lower reaches. Nowadays, the apex of the downstream loop (lower reach) seems to be more active and is migrating rapidly towards the upper reach. If the secondary channels in the lower reach do not increase their trapping efficiency (as it seems is happening now), the upper and lower reaches might collide in the near future.

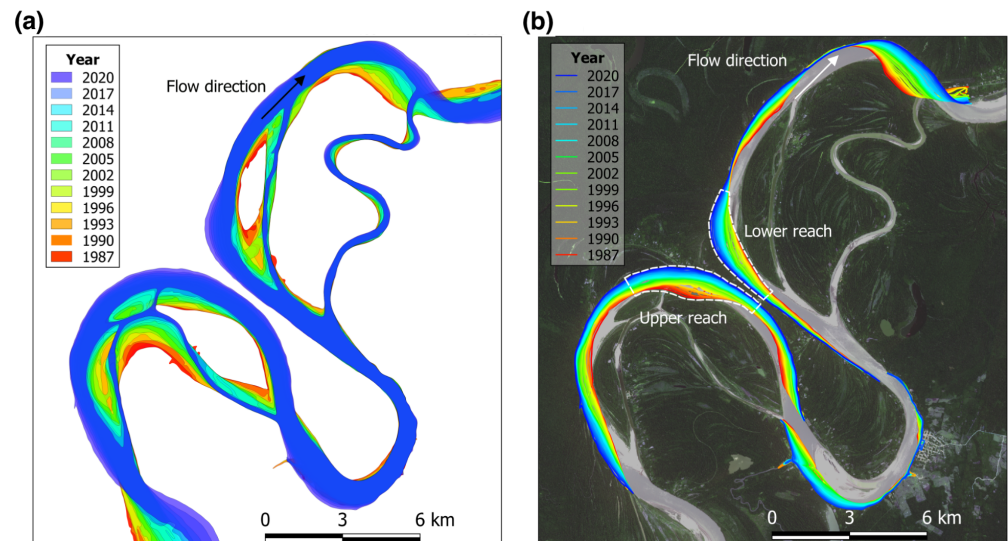


**Figure 3.** (a) Temporal (from 1987 to 2020) migration of the Jenaro Herrera (JH) bend (see Figure 1 for location). (b) Outer bank migration from 1987 to 2020.

### 2.3. Downstream (DS) Bend

The DS bend (Figure 4a) developed a cutoff processes between July and December 1996 (Figure 4b), when a small channel with a length of about one-ninth of the main channel width became incised on the downstream side of the meander loop, where the floodplain separated the two limbs by a distance of approximately 300 m, or about one-third of the main channel width. By June 1997, the cutoff process was completed, and the cutoff channel was approximately at full channel width.

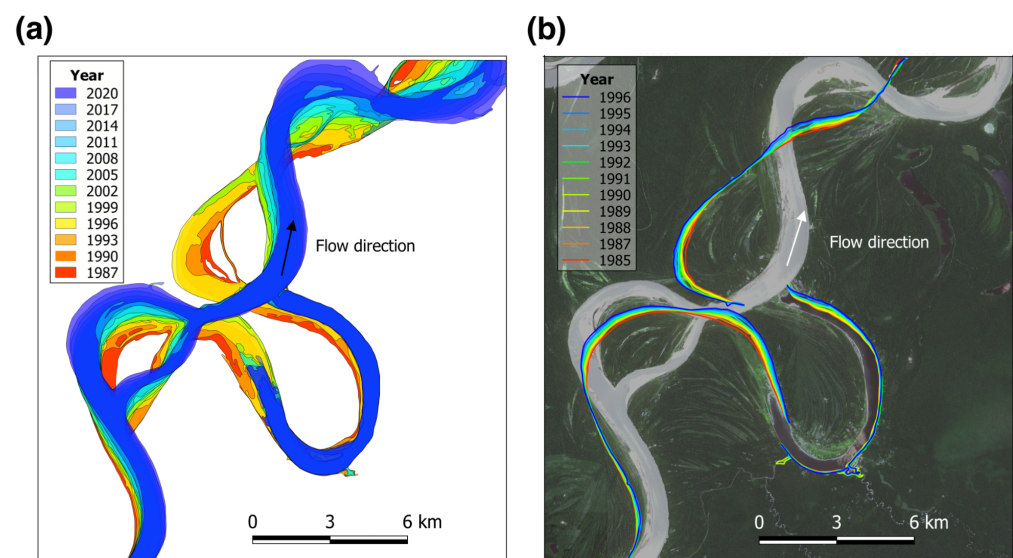


**Figure 4.** (a) Planform migration of the DS bend (see Figure 1 for location) from 1987 to 2020. (b) The migration of the outer bank from 1985 to 1996 when the neck cutoff occurred.

The bifurcation of the cutoff channel was near the bifurcation of secondary channel on the downstream reach of the bend, and after the cutoff channel had formed, the flow downstream of the cutoff was rerouted through the secondary channel, a path that reduced the sinuosity. The flood season of 1996 (from late January through June) produced water levels above the average of the season, particularly in the transitional stage from October through December, but the water level did not exceed the average by more than 1.7 m. This cutoff process may be explained by the mechanism described by [14], where a channel is incised from the downstream side of the loop over multiple flood seasons. Some of the highest water levels of the period of record, exceeding the daily average by more than 4.5 m at some points, happened during 1993 and 1994, where 1993 showed some of the highest recorded stages for almost the entire year, and 1994 had one of the highest recorded stages from the peak through the transition into the low season. The river water levels during the high seasons of 1995 and 1996 were lower compared to the ones of 1993 and 1994, but were still higher than average. It appears that there was a narrow channel across the loop by June 1994; during 1996, the new channel appeared on the downstream end of where this same channel was located.

#### 2.4. Migration Rates along the JH Bend

From the previous sections, both cutoffs (US and DS) appear to have occurred during the rising transition from the low to the high season. By the end of the high season, when the water level was decreasing, the new channel had been developed to full width and had become the preferred flow path. The US cutoff appears to have occurred in a year with unusually low flows during the high season and unusually high flows during the low season. This quick transition may have led to the contribution of less developed vegetation to the collision of the two reaches to form a new channel. The DS cutoff, however, was likely formed over a longer time period, but once the new channel was large enough to marginally connect the two limbs, the cutoff was completed in the same year. These two bends, US and DS, show typical migration patterns of meandering channels, where secondary channels did not interfere with the process; however, in the case of the JH bend, the presence of secondary channels along the upstream and downstream reaches is clearly modifying its planform dynamics. Therefore, herein, a closer look into the migration rates of the JH bend is presented. [30] estimated an average migration rate of 60 m/year at the apex of meanders in the lower Ucayali River and estimated that it would take from 100 to 200 years for a meander loop to form, however as described before, migration rates are modulated by the presence or absence of secondary channels. Herein, the migration rates were calculated for the period of study using mStaT toolbox [27]. The migration rates were calculated for the upper and lower reaches of the JH bend (Figure 1c). Average migration rates of the outer banks were calculated for each year in the period of study using the bank lines from the current and previous year.

The analysis shown in Figure 5 indicates that the upper reach has developed averaged migration rates higher than 10 m/year (from 1986 to 2019), while the lower reach has increased the averaged migration rates from 3 m/year to peaks of 42 m/year since 1992. Nowadays, it seems that both upstream and downstream bends from Jenaro Herrera town have similar amplitudes; thus, migration rates of the upper and lower reaches are similar, around 25 m/year by 2019. The distance between the two bends is decreasing, being less than 300 m by 2022. Based on migration rates of the three bends (US, DS and JH), it seems that the presence of secondary channels in the JH bend drastically reduces the migration rates of the most outer channels; therefore, the time that the JH bend is taking to produce a cutoff is longer than the US and DS bends. However, as described earlier, the secondary channels along the JH bend are decreasing their channel widths (Figure 3a), evidence of a reduction in trapping efficiency; thus, a reactivation of migration along the main channel is observed. Figure 1d shows the geomorphic reconstruction of the JH bend, where scroll bars, paloechannels and oxbow lakes are present in the floodplain, along with scroll bars, as observed in Figure 3b). Therefore, not only are planform migration rates important to define

when the upstream and downstream reaches might collide, it is also important that during high-flow events [2], the scroll bars and paleochannels can act as connecting channels that might incise and define the location where the upstream and downstream reaches of the bend may connect and not necessarily develop a cutoff by the collision of the channels. Consequently, a bend cutoff might occur under both alternatives. Therefore, detailed field measurements and hydrodynamic modeling was utilized to predict the potential neck cutoff in the JH bend.

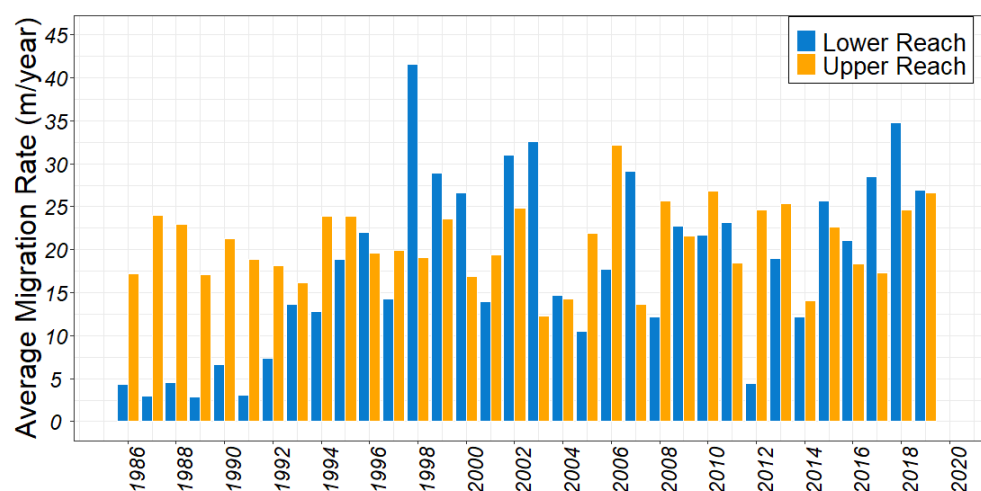


Figure 5. Migration rates for upper and lower reaches of the JH bend (see Figure 3b).

### 3. Field Measurements along the JH Bend

Figure 3 shows that the JH bend is under an imminent neck cutoff process; thus, to start monitoring and predicting the cutoff, field measurement campaigns were carried out in May and August of 2013 and February 2019. The field measurements covered high and low flow seasons (as observed in Figure 1e). Field measurements included bed morphodynamics (May 2013), hydrodynamics (May and August 2013, February 2019), and sediment transport (August 2013 and February 2019).

#### 3.1. Bed Morphodynamics

Bathymetry measurements were obtained along the entire bend during May 2013 at a spacing of 500 m at the upstream and downstream ends of the bend and at a spacing of 250 m in the JH bend (shown by Figure 6). Notice that the secondary channels (C1, C2 and C3) are elevated, as has been observed in anabranching channels [31].

#### 3.2. Hydrodynamics

Velocity measurements were taken at stations (four measurements per station) along the JH bend for May and August 2013 and February 2019 during field campaigns using an acoustic doppler current profiler (ADCP, Workhorse Rio Grande 600 KHz RD Instruments) and processed using the velocity mapping tool (VMT) [17,32]. The ADCP measurements for May and August 2013 are shown in Figure 7, where the letters “M” and “A” indicate the month the measurement was taken. The measurements for February 2019 are shown in Figure 8. For the case of May 2013, the higher velocities (therefore high shear stresses) are located closer to the outer bank (at M1, M2 and M3). The secondary flow is quite noticeable in M2, where the flow moves towards the outer bank near the water surface and towards the inner bank near the bed, showing a typical secondary flow (tangential vectors) at high-amplitude bends [33]. The velocities are higher near the outer bank for M2, indicating more potential for erosion; however, the adjacent geologic formation and higher elevation of the terrain (see Figure 1a,d) does not allow the Ucayali River to further migrate to the east, where the Jenaro Herrera town is located. The Ucayali River has reached the

valley edge near the Jenaro Herrera town, and as observed in Figure 6, the deepest bed erosion occurs just downstream of Jenaro Herrera town. As shown in Figure 3, Jenaro Herrera town might become isolated from the Ucayali River, while other small towns (that are located inside of the river valley) might undergo relocation due to planform migration processes. For the measurements of August 2013, the velocity distribution is similar to the case of May, with higher velocities towards the outer bank. It seems that even for low discharges, there are important velocity gradients that induce high shear stresses along the outer bank in the A1 and A5 stations.

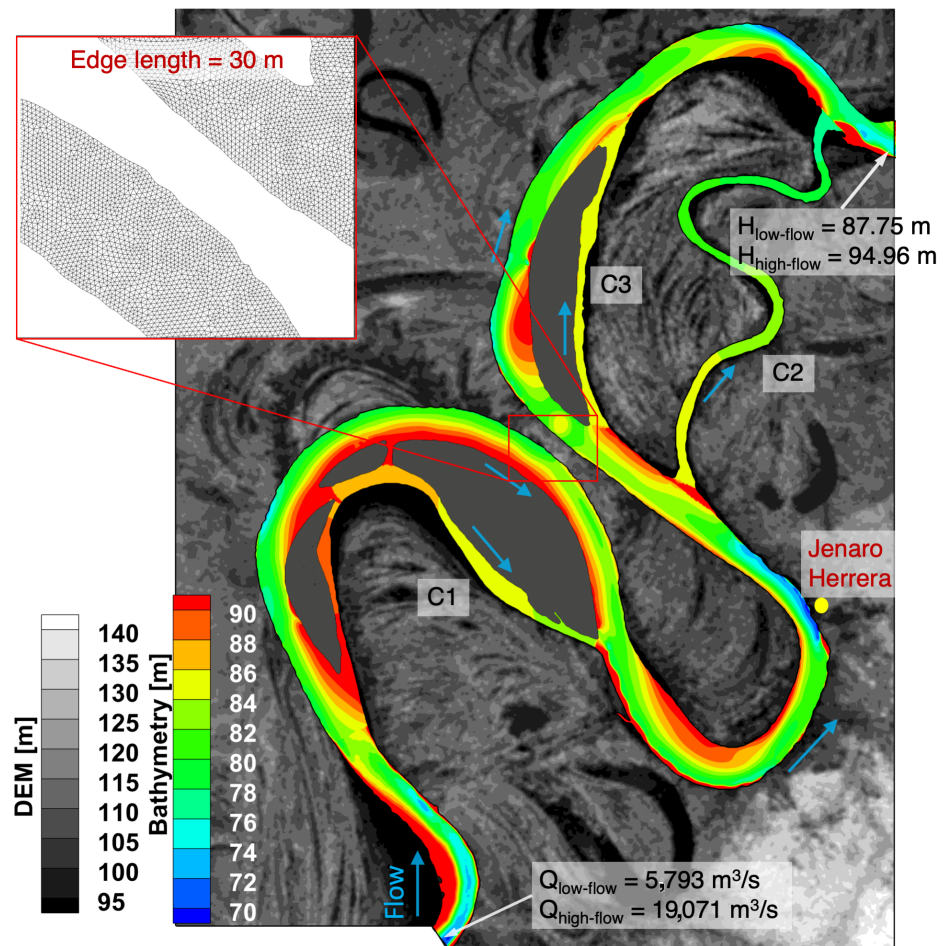


**Figure 6.** Bed elevation of the JH bend (May 2013).  $Q_{high-flow} = 19,071 \text{ m}^3/\text{s}$  and  $Q_{low-flow} = 5793 \text{ m}^3/\text{s}$  represent water discharges for May and August 2013, respectively.  $H_{high-flow} = 94.96 \text{ m}$  and  $H_{low-flow} = 87.75 \text{ m}$  represent water surface elevation for May and August 2013, respectively. Secondary channels C1, C2 and C3 are elevated channels.

Figure 8 shows the velocity measurements for February 2019. According to the flow hydrograph (Figure 1e), February's discharge is close to peak discharge (usually similar to May's and definitely higher than August's discharge); therefore, the velocity magnitude is higher, and the secondary flow (see velocity arrows) is stronger in all cross sections. At station 4 (close to Jenaro Herrera town), the bed topography presents a mid-bar deposition (see cross section 4 in Figure 8), and the flow is divided into left and right channels, where the higher velocity is concentrated towards the right channel. Indeed, station 5 does not represent a typical meandering bathymetry, since the transversal bed slope is very weak and the flow is redistributed across the section. Along the upper (stations 1, 2 and 3) and lower reaches (stations 9, 10, and 11), it seems that the lower reach presents stronger secondary cells and deeper outer bank scour holes ( $>25 \text{ m}$ ).

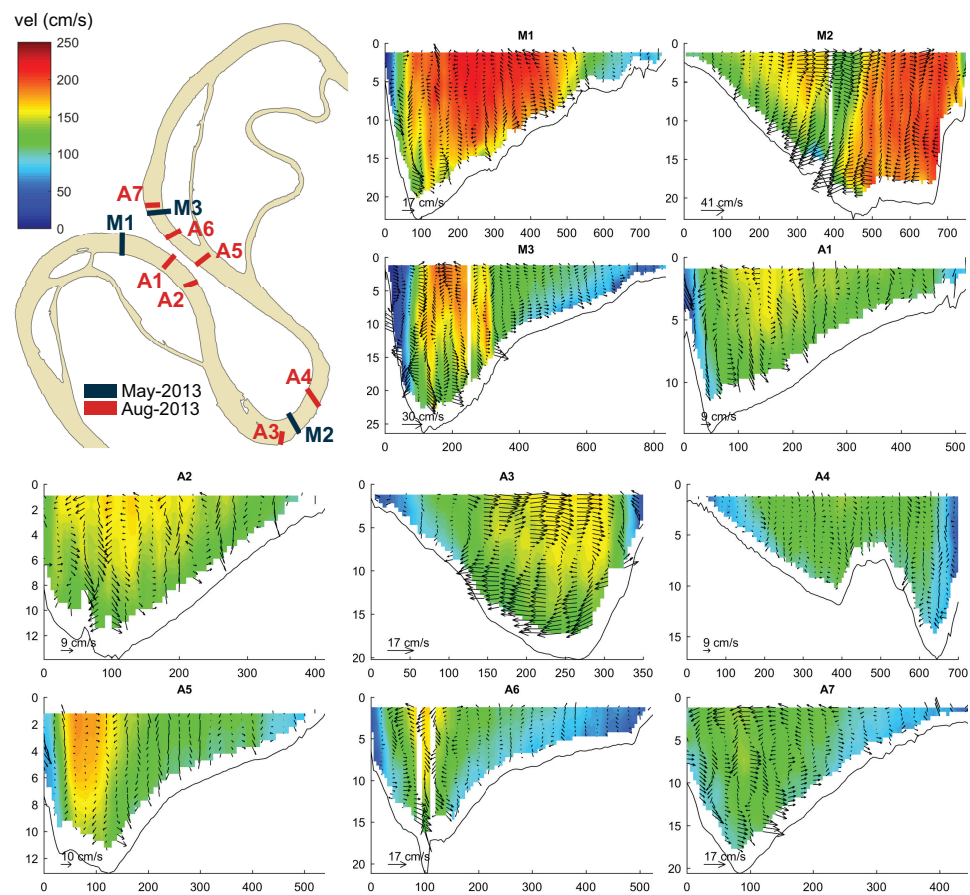
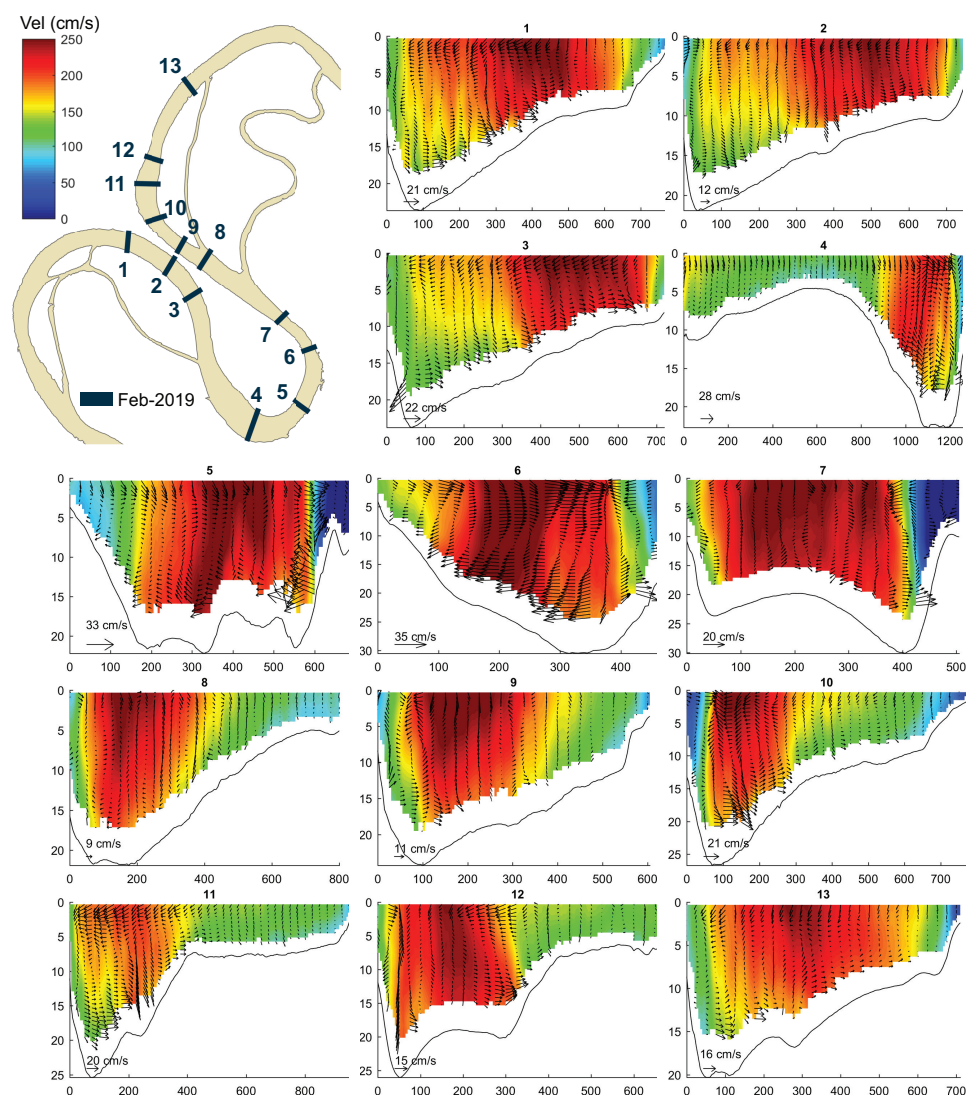


**Figure 7.** Velocity measurements of 2013 along the JH bend. The vectors represent the secondary flow using the Rozovskii decomposition, while the contours represent the velocity magnitude. M: May and A: August. May's water discharges ( $Q$  ( $\text{m}^3/\text{s}$ )) are 14,749.3 (M1), 17,034.6 (M2), and 12,999.4 (M3). August's water discharges ( $Q$  ( $\text{m}^3/\text{s}$ )) are 4947.4 (A1), 4670.3 (A2), 5449.8 (A3), 6018.5 (A4), 4745.4 (A5), 5162.7 (A6), and 5127.8 (A7).

### 3.3. Bed and Floodplain Sediment Characterization

Figure 9 shows the bed and floodplain sediment characterization for the JH bend. The sampling points at the main channel upstream Jenaro Herrera town are: S1-R, S1-C, S1-L, S2-C, S2-R, S3-L, S3-C, and S3-R; the sampling points at the floodplain are B-3m, F1, F2, F3, F4 and F5; and the sampling points downstream of Jenaro Herrera town at the main and secondary channels are: J1-L, J1-C, J1-R, J2-L, J2-C, J3-C and J4-C. Bed sediment samples along the main channel and floodplain (secondary channels) were collected in August 2013 (February 2019). Sediment concentrations (WL: wash load, SBM: suspended bed material) along the secondary channels were collected during February 2019. As observed in Figure 1, the bank material near Jenaro Herrera town belongs to an elevated tertiary formation; thus, the Ucayali River cannot migrate towards the east. Sediment samples along the floodplain were taken by penetration with a metallic pipe ( $\approx 50$  cm, see pictures). At station 1 (S1-R, S1-C, S1-L), the  $D_{50}$  sediment size at the inner and outer banks are 0.3 mm (S1-R) and 1.1 mm (S1-L), respectively. A similar trend of finer material at the inner bank is observed in station 2. At station 3, the difference between the bed material at the inner bank and outer bank are not noticeable, since that portion of the bend presents less curvature (to induce sediment redistribution) and is affected by secondary channels C2 and C3 (see Figure 6). The sediment distribution along the floodplain seems to be quite homogeneous, having a  $D_{50}$  of around 0.2 mm (deposited by flooding and historical planform migration of the Ucayali River). The sediment sample taken at 3 m above the water surface along the outer bank in station 1 (B3m, Figure 9) shows similar distribution as the surface floodplain samples (F1 to F5). The bed sediment size distribution for the

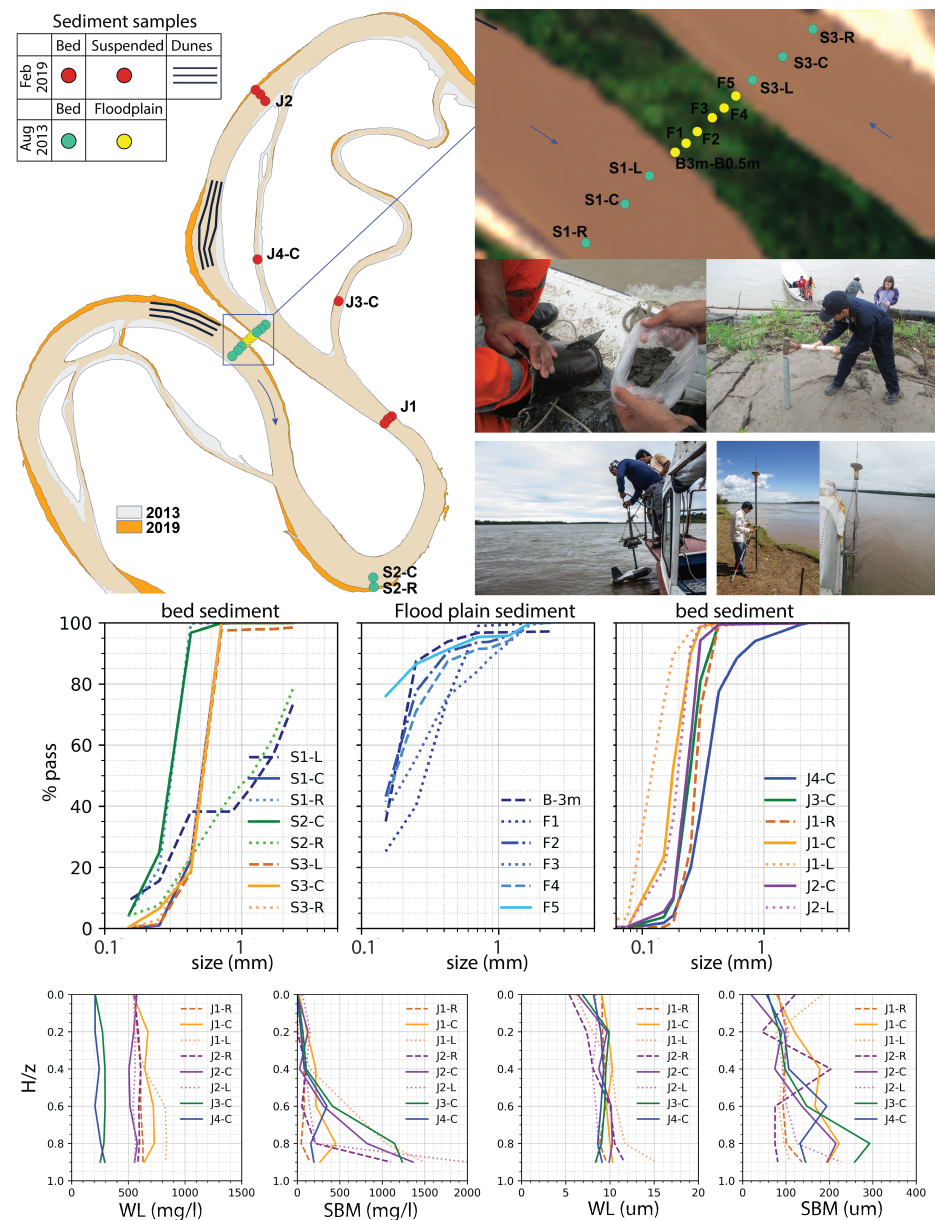
secondary channels shows that the  $D_{50}$  is around 0.2 mm, very similar to the sediment along the deposits along inner bank. As observed in Figure 6 (and similar to [34,35]), the bed elevation of the secondary channels are at a higher elevation than the main channel; therefore, most of the trapped sediments into secondary channels are finer material that is re-suspended into the water column. Thus, it is no surprise that the sediment size of the finer material (inner bank) along the main channel is similar to those along the secondary channels. Indeed, the sediment size distribution along the water column for the wash load has an almost homogeneous  $D_{50}$  of around 10 $\mu$ m, while the suspended bed material has a range of  $D_{50}$  between 20 (close to the surface) to 300  $\mu$ m (close to the bed). A similar trend is observed with the sediment concentration, which is homogeneous (1500 mg/L) for the wash load, while there is a slight stratification (from 1 to 1000 mg/L) for the suspended bed material.



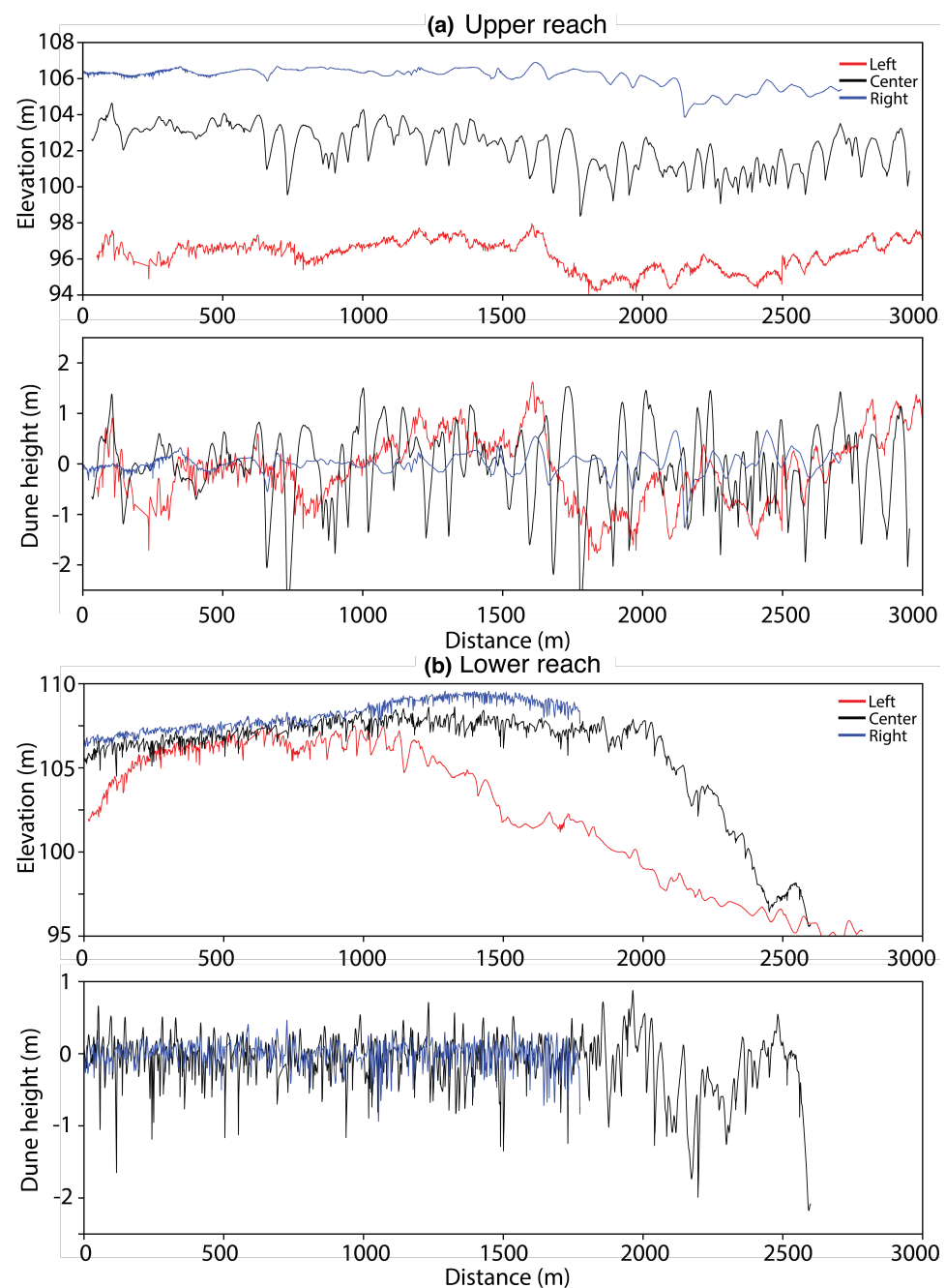
**Figure 8.** February 2019's velocity measurements along the JH bend. The vectors represent the secondary flow using the Rozovskii decomposition, while the contours represent the velocity magnitude. February's water discharges ( $Q$  ( $\text{m}^3/\text{s}$ )) are 18,825.8 (1), 18,900.3 (2), 18,682.5 (3), 19,541.6 (4), 19,256.8 (5), 19,331.3 (6), 19,471.3 (7), 17,521.5 (8), 16,642.3 (9), 16,392.4 (10), 16,257.8 (11), 16,148.3 (12), and 16,138.9 (13).

Figure 10 shows measurements of longitudinal (3 km) bed profiles at the upper and lower reaches (see black lines in Figure 9). For the upper reach, based on the difference between the left and right profile elevations ( $\approx 10$  m), there is an important transversal bed

slope, describing a typical depositional (erosional) region near the inner (outer) bank of the meandering channel. For the lower reach along the first km, not much difference between the left and right profiles is found (indicating a stronger depositional pattern or accretion at the inner bank); however, further downstream, the transversal bed slope increases due to a planform curvature change. In this reach, the transversal morphology is not as developed as in the upper reach. Finally, using the discretization method proposed by [36], the dune heights were estimated as  $\approx 2$  m, with larger size bedforms observed along the center of the channel, providing a larger localized bedform roughness.



**Figure 9.** Sediment characterization (location, sediment size distribution and suspended sediment concentration) along the JH bend (main channel (S1-R, S1-C, S1-L, S2-C, S2-R, S3-L, S3-C, and S3-R) and floodplain (B-3m, F1, F2, F3, F4 and F5) samples were collected in August 2013, while secondary channel (J1-L, J1-C, J1-R, J2-L, J2-C, J3-C and J4-C) samples were collected in February 2019). Pictures show the collection of suspended and floodplain sediments. WL: wash load; SBM: suspended bed material. Along the upper and lower reaches, three 3-km longitudinal profiles for bedform characterization were collected.



**Figure 10.** Bathymetry and dune height along three longitudinal profiles (left, center, and right) and dune heights (m) for: (a) upstream reach, (b) downstream reach (see Figure 9). The discretization of bedforms was obtained by using [36]’s methodology.

#### 4. Hydrodynamic Characteristics of the JH Bend

In order to correlate the planform migration and the occurrence of neck cutoff along the JH bend with the hydrodynamics, a numerical model was used. The model utilizes the two-dimensional depth-averaged hydrodynamic model TELEMAC-2D [37]. The  $k - \epsilon$  model was selected as the turbulence model, similarly to [31,34]. The downstream water surface elevation was obtained by interpolating Requena, Jenaro Herrera and Nauta stations, which are maintained by the Peruvian National Service of Meteorology and Hydrology (SENAMHI). Figure 6 shows the boundary conditions (discharge, water surface elevation at the downstream end, and bathymetry) of the computational domain. The discharge and water surface elevation boundary conditions are considered for both field measurements in 2013 (May and August). Therefore, velocities measured with ADCP were utilized to

calibrate the numerical model, and the friction coefficient of the bed was adjusted until the modeled velocities were similar to the ones measured in the field campaign. Additionally, the parameters of the secondary flow correction of two-dimensional depth were adjusted.

The water surface gradient and elevation were calibrated using information from the gauging stations. Figure 11 shows the comparison of measured and predicted depth-averaged velocities for May and August flow conditions. In general, the agreement is acceptable for a very large river like the Ucayali River. Similar hydrodynamic modeling was previously used in [31,34]. Notice that for May flow condition, the secondary channels can transport around 10% to 25% of the total water discharge, while for August’s flow condition, the water discharge in the secondary channels is negligible.

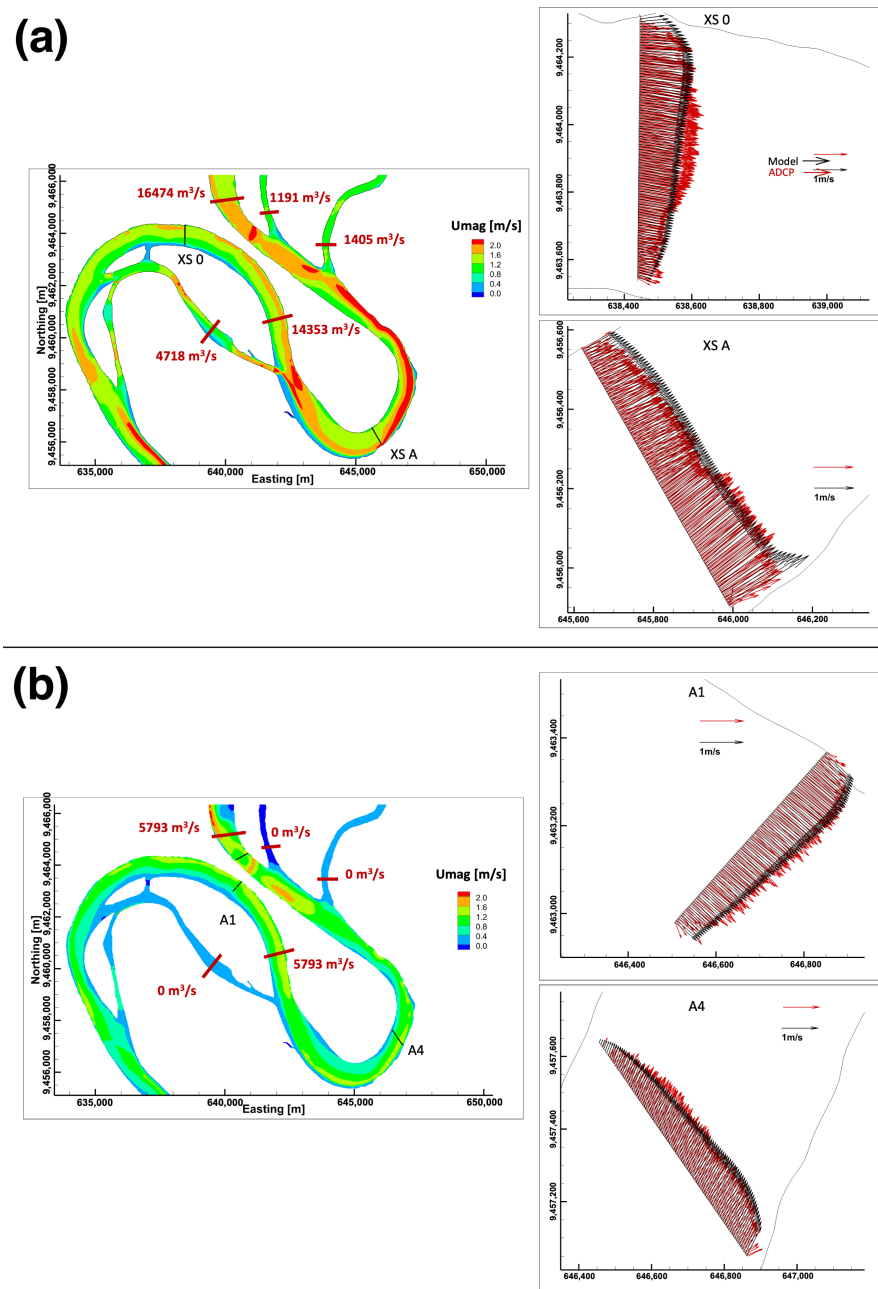


**Figure 11.** Comparison of measured and predicted depth-averaged velocities for: (a) May 2013 (stations XS0 and XSA) and (b) August 2013 (stations A1 and A2).

The hydrodynamic modeling indicates that high shear stresses are present around the upper and lower reaches (Figure 5), particularly during low flow conditions (Figure 12a,b).

Figure 12c,d shows the estimated bedload sediment transport rate (using [38]’s predictor) for high and low flows, respectively. It is clear that secondary channels are reducing their trapping efficiency (flow and sediment) and they might disappear in the near future, as in cases of the Amazon River [31]. The reduction in the size of the secondary channels increases the migration rates for the main channel.

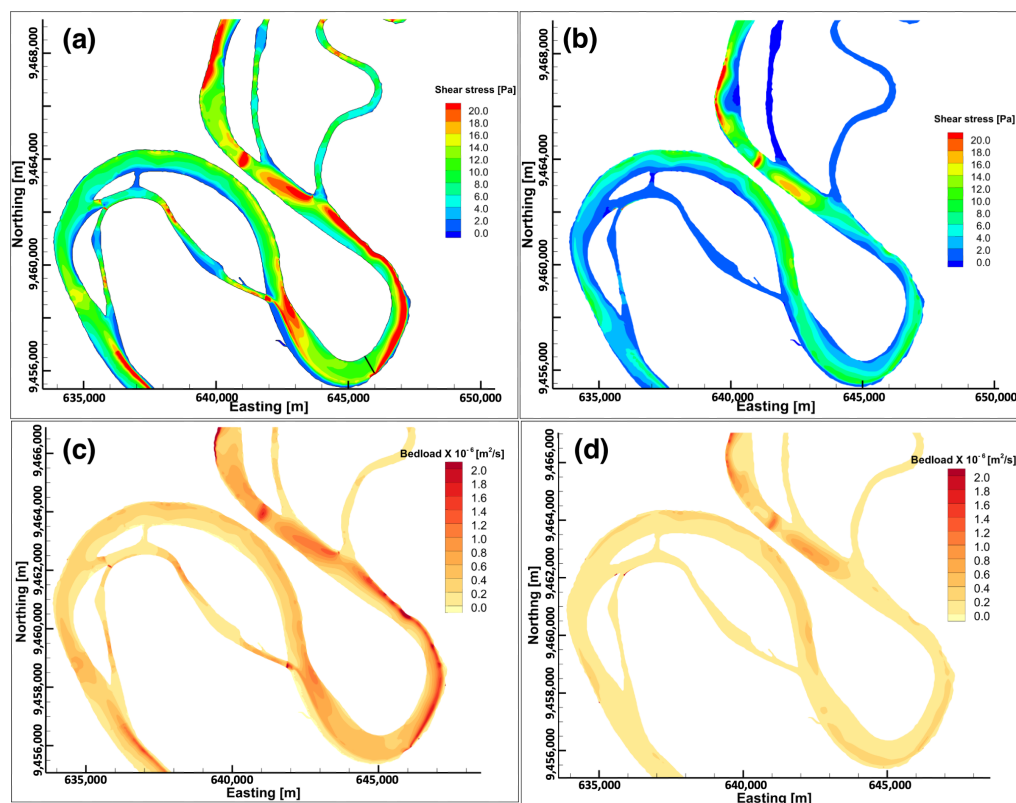


**Figure 12.** Shear stresses computed with the numeric model, (a) high flow conditions, (b) and low flow conditions. Bedload sediment transport rate, (c) high flow conditions, and (d) low flow conditions.

## 5. Discussion

The JH bend is a peculiar one since, as it is opposite to the US and DS bends, the existence of secondary channels changes the typical planform migration rates and patterns of single-thread meandering channels. Indeed, as observed in Figure 13, the channel C1 is modified from having a channel width of around 80% of the main channel in 1969 to having around 10% in 2020. C1 has changed due to the formation of islands I1, I2 and the slightly growing island I3 (Figure 13e). Channel C2 has not experienced important changes in planform migration and channel width; thus, the flow and sediment discharge into the C2 channel might be constant throughout the period of this analysis. Channel C3 did not change dramatically in planform shape (there is a small growth of island I4), but a reduction in channel width occurred, a consequence of a low velocity near the entrance of C3 and therefore the depositional zone, as observed in Figure 13g,h, respectively. The depositional zone at the entrance of C3 channel produces a slightly increment on flow velocities in the main channel (as observed in Figure 11). As discussed by [31,34], the morphodynamic interactions between secondary and main channels govern the flow and sediment redistribution in anabranching rivers. A similar behavior is found for transitional rivers, and the main channel is dominated by morphodynamic features of meandering channels.

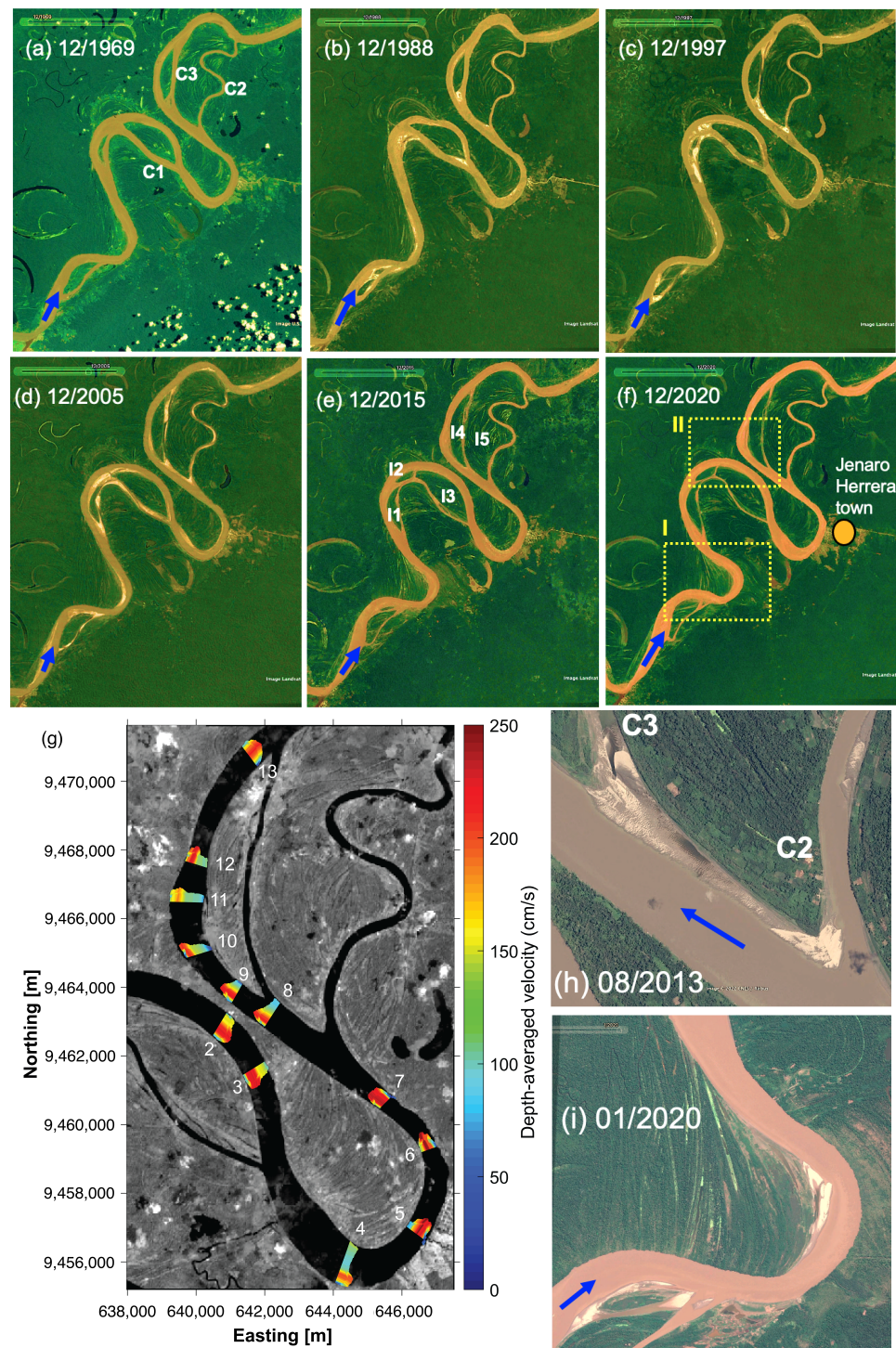


**Figure 13.** (a–f) Planform evolution of the JH bend from 1969 to 2020; (g) depth-averaged velocities for February 2019’s ADCP measurements; (h) depositional region at the entrance of the C2 channel and (i) upstream bend migration towards paleochannels and oxbow lakes.

Two potential regions for cutoff occurrence are identified in Figure 13f (yellow rectangles showing Migration I and II). The first region located upstream of JH bend (see in Figure 13i) shows a downstream migration of the entire bend. The second region is located downstream of the Jenaro Herrera Town (upper and lower reaches, Figure 5). Migration I shows a downstream migration of a bend that might collapse with oxbow lakes Sahuá and Supay, producing a cutoff through reconnecting oxbow lakes.

II was described extensively in the previous sections. Based on the planform analysis (Figure 3) and hydrodynamics modeling (Figure 11), planform migration II occurs somewhere around the closest region of the JH bend limps, since higher velocities (and higher shear stresses) develop near the river outer banks, particularly in the lower reach (see bed shear stresses in Figure 12b). Currently, the secondary channels are narrowing; with the potential development of a neck cutoff, it is probable that these secondary channels will be abandoned. If the secondary channels remain connected to the main channel, oxbow lakes will develop (similar conditions as the Sahuia and Supay lakes). The local economy relies on fish production. [25] mentioned a high correlation between complex morphology (including oxbow lakes) with fish production; thus, further research is needed to describe the socioeconomic impacts of planform changes. By either mechanism of cutoff (based on migration I or II) occurrence, several towns will be impacted by the planform migration of the Ucayali River. Jenaro Herrera town is located in an elevated area along the right river bank and probably will not suffer direct river erosion, but will be subject to river isolation if the Migration II scenario occurs. Smaller towns (see Figure 14) might need relocation considering the modified planform configuration. Relocation and affectation of river dynamics to towns occurs continuously in the Amazon basin, mainly related to flooding [39] and river migration [40].

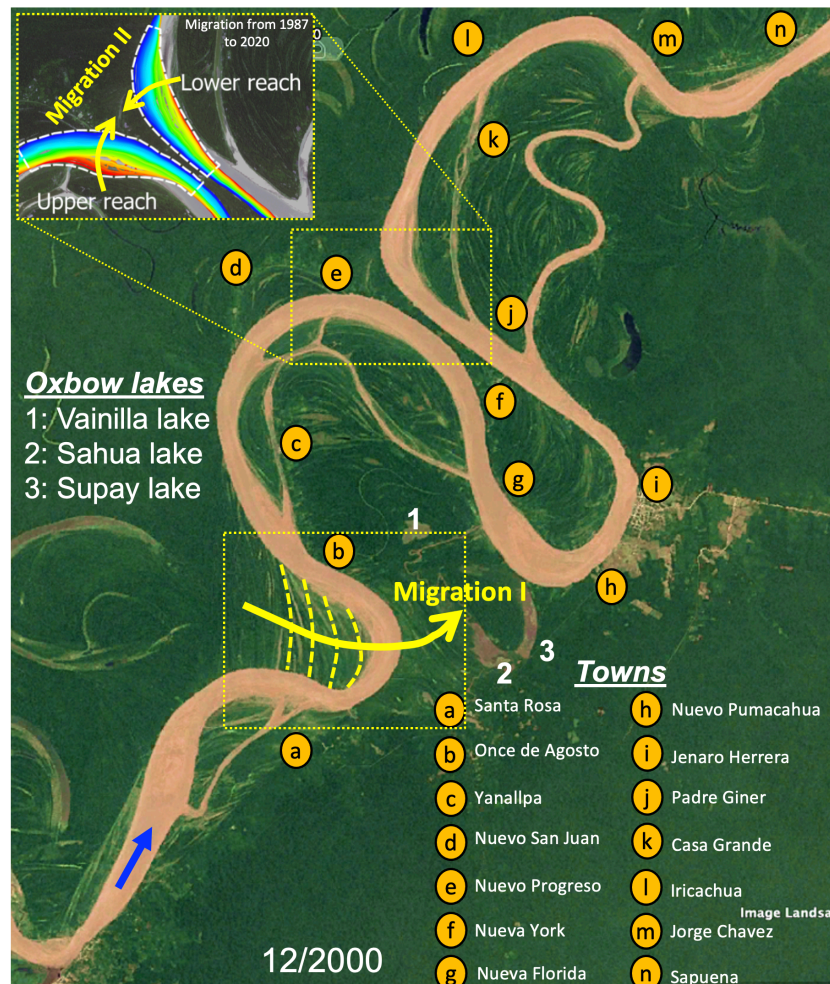


**Figure 14.** Towns (the location of towns were obtained from <https://fishbrain.com/> (accessed on 30 June 2022)), paleochannels and oxbow lakes surrounding Jenaro Herrera town. Notice that during the last years, two preferential migration directions are observed (Migration I: to merge into paleochannels and oxbow lakes, Migration II: to produce a neck cutoff).

## 6. Conclusions

The Ucayali River, one of the most active meandering rivers in the Amazon Basin, has average migration rates of 60–80 m/year. Here, the analysis of three bends of the river was performed. Two of them developed cutoff processes during the period of analysis, and the other, located near Jenaro Herrera town, is close to start a cutoff. Based on the analysis of planform evolution between 1987 and 2020, the The JH bend had a migration rate of 25 m/year, a smaller magnitude compared to average migration rates in the Ucayali River. The latter is due to the presence of secondary channels and islands that reduce and modify the flow and sediment redistribution, a similar process as in anabranching rivers [31, 34]. Two possible mechanisms of cutoff occurrence are described in the studied region (Migration I and II). Migration I might produce a cutoff through reactivation of oxbow lakes, while Migration II might happen based on a typical neck cutoff (where two bends collapse). Either mechanism will produce significant changes in the configuration of the entire JH bend (and sediment waves will produce erosional and depositional processes upstream and downstream of the cutoff location [24]). Long-term hydrogeomorphic monitoring (flow, sediment and bed and bank morphology) is necessary to: (1) understand where the cutoff and how the planform morphodynamic adaptation would occur near Jenaro Herrera town, (2) to develop socioeconomic planning based on town relocation (especially for small towns) and reconnection to the Ucayali River (especially for Jenaro Herrera town under the Migration II scenario), and (3) understand the effects of extreme events and climate change [41,42], and anthropic activities [43,44] into river dynamics.

**Author Contributions:** Conceptualization, J.D.A.; methodology, A.M., K.A., Z.T. and H.V.; software, A.M., G.M., C.F. and M.B.; validation, A.M., C.F. and M.B.; formal analysis, J.D.A. and A.M.; investigation, J.D.A., A.M., K.A. and Z.T.; resources, J.D.A. and A.M.; data curation, Z.T. and H.V.; writing—original draft preparation, J.D.A., A.M. and K.A.; writing—review and editing, Z.T., H.V., G.M., C.F. and M.B.; visualization, H.V., G.M. and A.M.; supervision, J.D.A.; project administration, J.D.A.; funding acquisition, J.D.A. All authors have read and agreed to the published version of the manuscript.

**Funding:** Thanks to the Gordon and Betty Moore Foundation for partially funding this study throughout the river characterization project in the Amazon River Basin (Grant GBMF7711, PI Dr. Abad).

**Data Availability Statement:** The data for the remote sensing analysis were obtained from <https://www.usgs.gov/centers/eros> (accessed on 30 June 2022).

**Acknowledgments:** Thanks to officers from the Peruvian Navy for assisting during the 2013 field measurements and to Jorge Paredes for the discussion on the hydraulics of the Ucayali River. Thanks to Bryan Santillan, Yulissa Estrada, Flor Fuentes, and Grecia Valdivia for assisting during the 2019 field measurements. Thanks to Marco Paredes from SENAMHI-Loreto for discussion on the hydrographs used for this study. The conceptual design of the field measurements and modeling scenarios were based on a collaboration between the Peruvian Navy and Abad's research group. Thanks to Jorge Bardales (deceased) from the Universidad Nacional de la Amazonia Peruana-UNAP who motivated students to perform research in Amazonian Rivers. The reviewers and editors are thanked for their wise comments and suggestions.

**Conflicts of Interest:** The authors declare no conflict of interest.

## References

1. Guyot, J.; Bazan, H.; Fraizy, P.; Ordonez, J.; Armijos, E.; Laraque, A. *Suspended Sediment Yields in the Amazon Basin of Peru: A First Estimation*; IAHS Publication: Wallingford, UK, 2007; pp. 3–10.
2. Guyot, C. Impact Socio-économique de la Migration des méandres du Fleuve Ucayali sur la Ville de Pucallpa. Master's Thesis, Université Aix-Marseille III, Marseille, France, 2007.
3. Goulding, M.; Barthem, R.; Ferreira, E. *The Smithsonian Atlas of the Amazon*; Smithsonian Books: Washington, DC, USA, 2003.
4. Puhakka, M.; Kalliola, R.; Rajasilta, M.; Salo, J. River Types, Site Evolution and Successional Vegetation Patterns in Peruvian Amazonia. *J. Biogeogr.* **1992**, *19*, 651–665. [[CrossRef](#)]

5. Wittmann, H.; von Blanckenburg, F.; Maurice, L.; Guyot, J.; Filizola, N.; Kubik, P.W. Sediment production and delivery in the Amazon River basin quantified by in situ-produced cosmogenic nuclides and recent river loads. *GSA Bull.* **2011**, *123*, 934–950. [[CrossRef](#)]
6. Parssinen, M.; Salo, J.; Räsänen, M.E. River Floodplain Relocations and the Abandonment of Aborigine Settlements in the Upper Amazon Basin: A Historical Case Study of San Miguel de Cunibos at the Middle Ucayali River. *Geoarcheology* **1996**, *11*, 345–359. [[CrossRef](#)]
7. Lathrap, D. Aboriginal occupation and changes in river channel on the central Ucayali, Peru. *Am. Antiq.* **1968**, *33*, 62–79. [[CrossRef](#)]
8. Lamotte, S. Fluvial dynamics and succession in the lower Ucayali River Basin, Peruvian Amazonia. *For. Ecol. Man.* **1990**, *33–34*, 141–156. [[CrossRef](#)]
9. Salonen, M.; Toivonen, T.; Cohalan, J.; Coomes, O. Critical distances: Comparing measures of spatial accessibility in the riverine landscapes of Peruvian Amazonia. *Appl. Geogr.* **2011**, *32*, 501–513. [[CrossRef](#)]
10. Frascati, A.; Lanzoni, S. Morphodynamic regime and long-term evolution of meandering rivers. *J. Geophys. Res. Earth Surf.* **2009**, *114*. [[CrossRef](#)]
11. Camporeale, C.; Perucca, E.; Ridolfi, L. Significance of cutoff in meandering river dynamics. *J. Geophys. Res. Earth Surf.* **2008**, *113*. [[CrossRef](#)]
12. Gagliano, S.; Howard, P. The neck cutoff oxbow lake cycle along the Lower Mississippi River. In *River Meandering*; Elliot, C., Ed.; ASCE: Reston, VA, USA, 1984; pp. 147–158.
13. Howard, A.; Knutson, T. Sufficient conditions for river meandering: A simulation approach. *Water Resour. Res.* **1984**, *20*, 1659–1667. [[CrossRef](#)]
14. Gay, G.; Gay, H.; Gay, W.; Martinson, H.; Meade, R.; Moody, J. Evolution of cutoffs across meander necks in Powder River, Montana, USA. *Earth Surf. Process. Landforms* **1998**, *23*, 651–662. [[CrossRef](#)]
15. Howard, A. Modelling channel evolution and floodplain morphology. In *Floodplain Processes*; Anderson, M., Walling, D., Bates, P., Eds.; Wiley: Hoboken, NJ, USA, 1996; pp. 15–62.
16. Lewis, G.; Lewin, J. Alluvial cutoffs in Wales and the Borderlands. *Mod. Anc. Fluv. Syst.* **1983**, *6*, 145–154.
17. Zinger, J.; Rhoads, B.; Best, J.; Johnson, K. Flow structure and channel morphodynamics of meander bend chute cutoffs: A case study of the Wabash River, USA. *J. Geophys. Res. Earth Surf.* **2008**, *118*, 2468–2487. [[CrossRef](#)]
18. Hudson, P.; Kesel, R. Channel migration and meander-bend curvature in the lower Mississippi River prior to major human modification. *Geology* **2000**, *28*, 531–534. [[CrossRef](#)]
19. Abizaïd, C. An anthropogenic meander cutoff along the Ucayali River, Peruvian Amazon. *Geogr. Rev.* **2005**, *95*, 122–135.
20. Coomes, O.; Abizaïd, C.; Lapoint, M. Human Modification of a Large Meandering Amazonian River: Genesis, Ecological and Economic Consequences of the Masisea Cutoff on the Central Ucayali, Peru. *Ambio* **2009**, *38*, 130–134. [[CrossRef](#)]
21. Quintana-Cobo, I.; Moreira-Turcq, P.; Cordeiro, R.C.; Aniceto, K.; Crave, A.; Fraizy, P.; Moreira, L.S.; de Aguiar Duarte Contrera, J.M.; Turcq, B. Dynamics of floodplain lakes in the Upper Amazon Basin during the late Holocene. *Comptes Rendus Geosci.* **2018**, *350*, 55–64. [[CrossRef](#)]
22. Schwenk, J.; Khandelwal, A.; Fratkin, M.; Kumar, V.; Foufoula-Georgiou, E. High spatiotemporal resolution of river planform dynamics from Landsat: The RivMAP toolbox and results from the Ucayali River. *Earth Space Sci.* **2017**, *4*, 46–75. [[CrossRef](#)]
23. Schwenk, J.; Foufoula-Georgiou, E. Are process nonlinearities encoded in meandering river planform morphology? *J. Geophys. Res. Earth Surf.* **2017**, *122*, 1534–1552. [[CrossRef](#)]
24. Abad, J.D.; Montoro, H.; Frias, C.; Paredes, J.; Peralta, B. The meandering Ucayali River, a cyclic adaptation of cutoff and planform migration. *River Flow Proc. Int. Conf. Fluv. Hydraul.* **2012**, *1*, 523–527.
25. Rojas, T.V.; Santillan, B.; Frias, C.E.; Abad, J.D. The hydro-geomorphological connectivity in the Ucamara Depression: The Pacaya-Samiria Wetland. In Proceedings of the AGU Fall Meeting Abstracts, New Orleans, LA, USA, 13–17 December 2021.
26. Guerrero, L.; Flores, G.; Valverde, H.; Chicchon, H.; Estrada, Y.; Naito, K.; Ortals, C.; Canas, C.; Abad, J.D. The birthplace of the Amazon River, a confluence of meandering and anabranching rivers. In Proceedings of the American Geophysical Union, Fall Meeting, San Francisco, CA, USA, 9–13 December 2019.
27. Ruben-Dominguez, L.; Naito, K.; Gutierrez, R.; Szupiany, R.; Abad, J.D. Meander Statistics Toolbox (MStAT): A toolbox for geometry characterization of bends in large meandering channels. *SoftwareX* **2021**, *14*, 100674. [[CrossRef](#)]
28. Brice, J. Evolution of meander loops. *Geol. Soc. Am. Bull.* **1974**, *85*, 581–586. [[CrossRef](#)]
29. Martinez, W.; Diaz, G.; Romero, L.; Morales, M.; Milla, D.; Raymundo, T.; Montoya, C.; Huayhua, J. *Geología de los Cuadrángulos de Bolívar, Curaray, Santa Clotilde, Quebrada Aguablanca, Quebrada Sabaloyacu, San Lorenzo, Intuto, Río Pintoyacu, Río Mazán, Río Corrientes, Libertad, Río Nanay, Santa Rosa, Yacumama, Río Itaya, Yanayacu, Chapajilla y Nauta*—[Boletín A 131]; INGEMMET. Boletín, Serie A: Carta Geológica Nacional, No. 131; Instituto Geológico, Minero y Metalúrgico: Lima, Peru, 1999; pp. 1–372.
30. Schumm, S.; Dumont, J.; Holbrook, J. *Active Tectonics and Alluvial Rivers*; Cambridge University Press: Cambridge, UK, 2000.
31. Mendoza, A.; Abad, J.D.; Frias, C.E.; Collin, O.; Paredes, J.; Montoro, H.; Vizcarra, J.; Simon, C.; Soto-Cortes, G. Planform dynamics of the Iquitos anabranching structure in the Peruvian Upper Amazon River. *Earth Surf. Process. Landforms* **2016**, *41*, 961–970. [[CrossRef](#)]

32. Parsons, D.; Jackson, P.; Czuba, J.; Engel, F.; Rhoads, B.; Oberg, K.; Best, J.; Mueller, D.; Johnson, K.; Riley, J. Velocity Mapping Toolbox (VMT): A processing and visualization suite for moving-vessel ADCP measurements. *Earth Surf. Process. Landforms* **2013**, *38*, 1244–1260. [[CrossRef](#)]
33. Abad, J.D.; Frias, C.E.; Buscaglia, G.C.; Garcia, M.H. Modulation of the flow structure by progressive bedforms in the Kinoshita meandering channel. *Earth Surf. Process. Landforms* **2013**, *38*, 1612–1622. [[CrossRef](#)]
34. Frias, C.E.; Abad, J.D.; Mendoza, A.; Paredes, J.; Ortals, C.; Montoro, H. Planform evolution of two anabranching structures in the Upper Peruvian Amazon River. *Water Resour. Res.* **2015**, *51*, 2742–2759. [[CrossRef](#)]
35. Mendoza, A.; Abad, J.D.; Langendoen, E.; Wang, D.; Tassi, P.; Abderrezzakk, E.K. Effect of sediment transport boundary conditions on the numerical modeling of bed morphodynamics. *J. Hydraul. Eng.* **2016**, *143*, 04016099. [[CrossRef](#)]
36. Gutierrez, R.; Abad, J.; Parsons, D.; Best, J. Discrimination of bedforms scales using robust spline and wavelet transforms: Methods and application to Synthetic Signals and the Parana River, Argentina. *J. Geophys.-Res.-Earth-Surf.* **2013**, *118*, 1400–1419. [[CrossRef](#)]
37. Lang, P. *Telemac-2d User's Manual*; Technical Report; Tech. Rep. EDF R & D: Paris, France, 2013.
38. Wong, M.; Parker, G. Reanalysis and correction of bed-load relation of Meyer-Peter and Muller using their own database. *J. Hydraul. Eng.* **2006**, *132*, 1159–1168. [[CrossRef](#)]
39. Bergmann, J. Planned relocation in Peru: Advancing from well-meant legislation to good practice. *J. Environ. Stud. Sci.* **2021**, *11*, 365–375. [[CrossRef](#)]
40. Nagel, G.W.; de Moraes Novo, E.M.L.; Martins, V.S.; Campos-Silva, J.V.; Barbosa, C.C.F.; Bonnet, M.P. Impacts of meander migration on the Amazon riverine communities using Landsat time series and cloud computing. *Sci. Total Environ.* **2022**, *806*, 150449. [[CrossRef](#)]
41. Marengo, J.A.; Souza, C.M.; Thonicke, K.; Burton, C.; Halladay, K.; Betts, E.A.; Alves, L.; Soares, W. Changes in climate and land use over the Amazon Region: Current and future variability and trends. *Front. Earth Sci.* **2018**, *21*, 228. [[CrossRef](#)]
42. Nobre, C.A.; Sampaio, G.; Borma, L.S.; Castilla-Rubio, J.C.; Silva, J.S.; Cardoso, M. Land-use and climate change risks in the Amazon and the need of a novel sustainable development paradigm. *Proc. Natl. Acad. Sci. USA* **2016**, *113*, 10759–10768. [[CrossRef](#)] [[PubMed](#)]
43. Amaral e Silva, A.; Braga, M.Q.; Ferreira, J.; Juste dos Santos, V.; do Carmo Alves, S.; de Oliveira, J.C.; Calijuri, M.L. Anthropogenic activities and the Legal Amazon: Estimative of impacts on forest and regional climate for 2030. *Remote Sens. Appl. Soc. Environ.* **2020**, *18*, 100304. [[CrossRef](#)]
44. Spracklen, D.V.; Garcia-Carreras, L. The impact of Amazonian deforestation on Amazon basin rainfall. *Geophys. Res. Lett.* **2015**, *42*, 9546–9552. [[CrossRef](#)]